Nuclear Instruments and Methods in Physics Research B 309 (2013) 183–188

Contents lists available at SciVerse ScienceDirect

Nuclear Instruments and Methods in Physics Research B

journal homepage: www.elsevier.com/locate/nimb

SPARC_LAB present and future

M. Ferrario [a,*], D. Alesini [a], M. Anania [a], A. Bacci [a], M. Bellaveglia [a], O. Bogdanov [a], R. Boni [a], M. Castellano [a], E. Chiadroni [a], A. Cianchi [a], S.B. Dabagov [a], C. De Martinis [a], D. Di Giovenale [a], G. Di Pirro [a], U. Dosselli [a], A. Drago [a], A. Esposito [a], R. Faccini [a], A. Gallo [a], M. Gambaccini [a], C. Gatti [a], G. Gatti [a], A. Ghigo [a], D. Giulietti [a], A. Ligidov [a], P. Londrillo [a], S. Lupi [a], A. Mostacci [a], E. Pace [a], L. Palumbo [a], V. Petrillo [a], R. Pompili [a], A.R. Rossi [a], L. Serafini [a], B. Spataro [a], P. Tomassini [a], G. Turchetti [a], C. Vaccarezza [a], F. Villa [a], G. Dattoli [b], E. Di Palma [b], L. Giannessi [b], A. Petralia [b], C. Ronsivalle [b], I. Spassovsky [b], V. Surrenti [b], L. Gizzi [c], L. Labate [c], T. Levato [c], J.V. Rau [c]

[a] INFN, Via E. Fermi, 40 00044 Frascati, Roma, Italy
[b] ENEA C.R. Frascati, Via E. Fermi, 45 00044 Frascati, Roma, Italy
[c] ILIL, INO-CNR, Via Moruzzi, 1 56124 Pisa Italy

ARTICLE INFO

Article history:
Received 21 December 2012
Received in revised form 25 March 2013
Accepted 25 March 2013
Available online 15 April 2013

Keyword:
Advanced accelerator concepts

ABSTRACT

A new facility named SPARC_LAB has been recently launched at the INFN National Laboratories in Frascati, merging the potentialities of the former projects SPARC and PLASMONX. We describe in this paper the status and the future perspectives at the SPARC_LAB facility.

1. Introduction

A new facility named SPARC_LAB (Sources for Plasma Accelerators and Radiation Compton with Lasers and Beams) has been recently launched at the INFN National Laboratories in Frascati, merging the potentialities of the former projects SPARC [1] and PLASMONX [2]. Ten years ago in fact, a robust R&D program on ultra-brilliant electron beam photoinjector and on FEL physics, the SPARC project, collaboration among INFN, ENEA and CNR, was approved by the Italian Ministry of Research and located at the INFN National Laboratories in Frascati.

The test facility is now operating, hosting a 150 MeV high brightness electron beam injector [3], able to operate also in the velocity bunching configuration [4], which feeds a 12 m long undulator. Observations of FEL radiation in the SASE [5], Seeded [6] and HHG [7] modes have been performed from 500 nm down to 40 nm wavelength. A second beam line has been also installed and is now hosting a narrow band THz radiation source [8]. In parallel to that, INFN decided to host a 200 TW laser that will be linked to the linac and devoted to explore laser-matter interaction, in particular with regard to laser-plasma acceleration of electrons [9] (and protons) in the self injection and external injection modes. The facility will be also used for particle driven plasma acceleration experiments, the COMB [10] experiment. A Thomson back-scattering experiment coupling the electron bunch to the high-power laser to generate a quasi coherent, monochromatic X-ray radiation is also in the commissioning phase. An upgrade of the linac energy up to 200 MeV is also foreseen by the end of 2013 by installing two new high gradient C-band structures developed at LNF in the framework of the ELI_NP collaboration [18]. A layout of the facility is shown in Fig. 1.

2. High power laser system

The SPARC_LAB high power laser system, named FLAME, has been recently fully commissioned. FLAME is based upon a Ti:Sa, chirped pulse amplification (CPA) laser able to deliver up to 220 TW laser pulses, 25 fs long, with a 10 Hz repetition rate at a fundamental wavelength of 800 nm, see Fig. 2.

The system features are characterized by a high contrast ratio (>10^{10}) and a fully remotely controlled operation mode. It includes a front-end with pulse contrast enhancement, bandwidth control and regenerative amplifier and yields pulses with 0.7 mJ in 80 nm bandwidth. These pulses are then further amplified by the first amplifier up to 25 mJ while the second amplifier brings the

* Corresponding author.
E-mail address: massimo.ferrario@lnf.infn.it (M. Ferrario).

0168-583X/$ - see front matter © 2013 Elsevier B.V. All rights reserved.
http://dx.doi.org/10.1016/j.nimb.2013.03.049

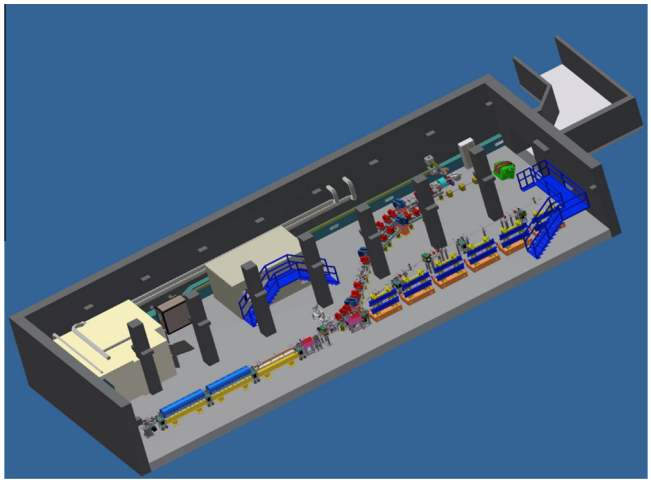

Fig. 1. Layout of the SPARC_LAB facility.

energy up to 600 mJ. The third cryogenic amplifier is based on a 50 mm Ti:Sa crystal pumped by 10 frequency doubled Nd:YAG laser pulses, reaching an energy up to 20 J at 532 nm. The extraction energy is as high as 35%, leading to a final energy in the stretched pulses in excess of 7 J. The pulse is then compressed to minimum pulse duration below 30 fs. Once compressed, the pulse is transported under vacuum to the target area via remotely controlled beam steering mirrors. For typical experimental conditions of laser wakefield acceleration in self-injection configuration, the laser pulse is focused at peak intensities exceeding 10^{18} W/cm^2 which, with our ASE contrast, gives a precursor laser intensity on a target below 10^9 W/cm^2. In the case of interaction with gases at pressures ranging from 1 to 10 bar, this laser intensity is below the plasma formation threshold for laser pulses of sub-nanosecond duration, which is typical duration of the ASE pulses. Therefore, we can reasonably assume that, in the case of interaction with gases, no premature plasma formation occurs and the CPA pulse can be focused directly in the gas.

Among the different uses of FLAME, the scientific program includes self-injection and external injection [19] experiments and the realization of an X-ray source based on the Thomson backscattering process. To this purpose, a careful characterization of FLAME performances with particular reference to the transverse beam quality was carried out during the commissioning. The measured Strehl ratio is greater than 50% up to pulse energies of approximately 6 J. For energies between 6 and 7 J, the phase front distortion increases leading to the reduction of the Strehl ratio to a minimum value of 35%. Our measurements show that the phase front pattern remains very stable from shot to shot at a given pulse energy. This makes the phase front correction with adaptive optics (planned for installation by the end of 2013) a reliable and complete solution to achieve a high quality focal spot.

3. Thomson source

The Thomson back-scattering (TS) X-ray source [11] is foreseen to work in three different operating modes: the high-flux- moderate-monochromaticity-mode (HFM2), suitable for medical imaging, the moderate-flux- monochromatic-mode (MFM) suitable to improve the detection/dose performance [12,13] and the short-and-monochromatic-mode (SM) useful for pump-and-probe experiments e.g., in physical-chemistry when tens of femtosecond long monochromatic pulses are needed.

The installation of the beamline will be completed by the 2013 summer with a transfer line for the electron beam together with a photon beamline that brings the laser pulse from the FLAME target area to the interaction with the electron beam. In this configuration the electron beam energy can range from 28 MeV to 150 MeV, and the electron beam transport is meant to preserve the high brightness coming from the linac and to ensure a very tight focusing and a longitudinal phase space optimization for the whole energy span. The general layout is showed in Fig. 3, where the electron transfer line departs from a three way vacuum chamber inside the first dipole downstream the RF deflector used for the six-dimensional phase space analysis of the electron beam. This dipole is also part of the 14° dogleg that brings the electron beam up to the SPARC THz source.

The electron beamline continues in a 30 m double dogleg starting, as mentioned, downstream the SPARC photoinjector; they ends in a two branch beam delivery line that provides two separate interaction regions with the possibility to host two different experiments at the same time: the Thomson source and the external injection in a plasma accelerator experiment. The total beam deflection is about 6 m from the photoinjector and undulator axes. A total of six rectangular dipoles and 19 quadrupoles

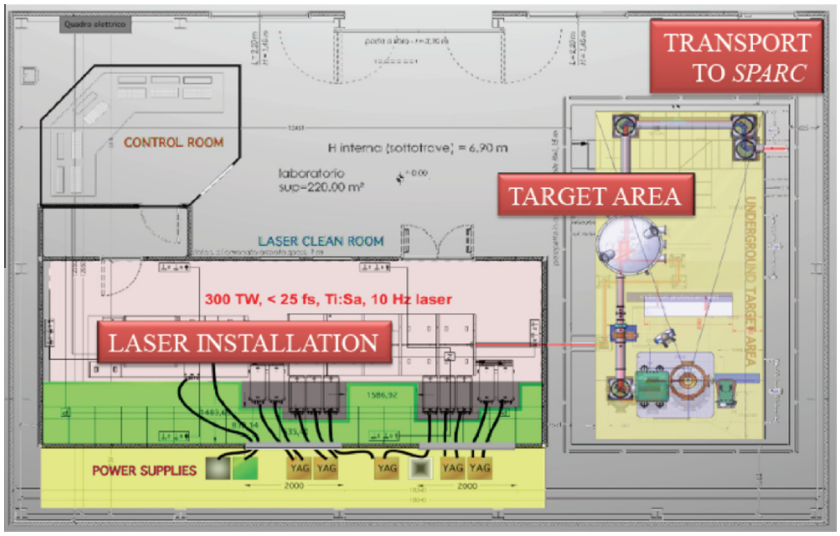

Fig. 2. Layout of the FLAME laser with the target area for self-injection plasma acceleration experiments.

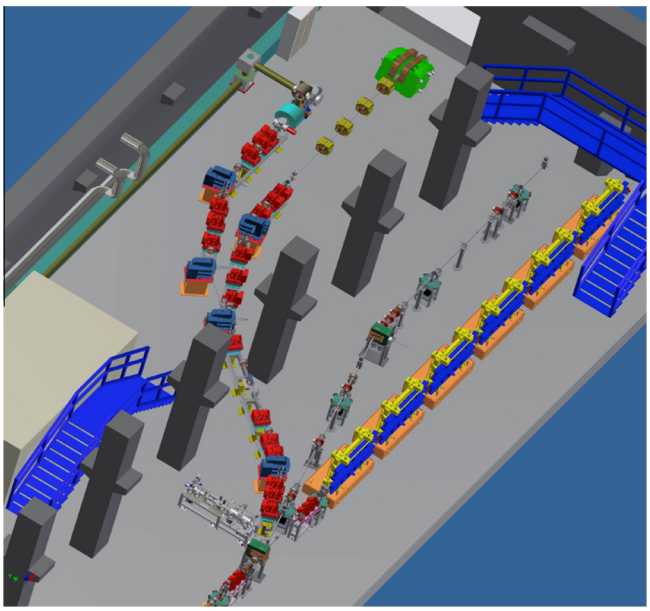

Fig. 3. Details of the SPARC_LAB facility showing present electron beam lines, downstream the injector from right to left: FEL undulators, THz source, Plasma Acceleration experiments, Thomson backscattering source.

are needed to drive the electron beam up to the two interaction points.

The Thomson interaction vacuum chamber, see Fig. 4, consists in two mirror stations that will determine the in and out trajectory of photon beam, plus an interaction chamber in the middle that hosts the diagnostic for both electron and photon beams. The parabolic mirror located downstream the interaction point will focus the photon beam at the interaction point down to a 10 μm spot size, its spatial adjustment is obtained with its x–y movable support that can be also remotely controlled. The interaction chamber is a tee-vacuum chamber where a double screen movement will be mounted to get the imaging of both electron and photon beams at the interaction point.

The laser beam transfer line to the interaction region is composed by a series of high reflectivity mirrors inserted in a vacuum pipe 50 m long. The mirrors, 8 inches diameter, are supported by motorized Gimbal mounts in order to assure the alignment up to the off-axis parabola that focus the laser pulse on the electron beam. The vacuum of the photon beam line is about 10^{-6} Torr.

The Thomson scattering experiment needs an extremely precise synchronization between electron bunch and laser pulse. The relative time of arrival jitter of two beams is fundamental to obtain a repeatable and efficient interaction. The electrons and photons have to be synchronized with a relative jitter <500 fs.

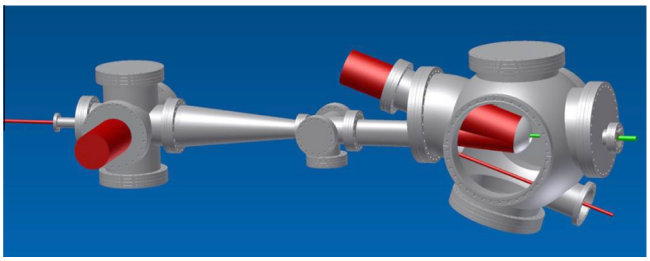

Fig. 4. Final drawing of the Thomson scattering interaction chamber.

4. Synchronization

In order to achieve specified performances of the next future experiments at SPARC_LAB a very demanding synchronization between the subsystems is required. In particular, two laser systems (SPARC photocathode and FLAME) have to be synchronized with a relative time jitter of <500 fs_{RMS} and <30 fs_{RMS} for the Thomson X-ray source and Plasma acceleration experiments, respectively.

The synchronization reference is presently distributed through coaxial cables along the facility. The measured performances fully meet the Thomson experiment requirements. Fig. 5 shows the schematics of the hardware configuration that synchronizes the two laser oscillators (and consequently the electron bunch and the FLAME amplified pulse at 10 Hz rep. rate).

Two Phase Locked Loops working at 2856 MHz (the SPARC linac frequency, equal to the 36th harmonics of the rep rate of the lasers) represented by the green boxes are used to independently synchronize two laser oscillators to the RF reference with a time jitter <100 fs_{RMS}.

The harmonic loop could lock the two lasers at any of 36 different relative time separations within one period of the laser rep rate T_{Las} = 12.6 ns. To select only one lock position and reject the others we added an ancillary PLL working at the laser fundamental frequency (orange boxes). This acts on the error amplifier of one harmonic loop opening a time window whose duration is only 1/36 of T_{Las}. A 360° electronic phase shifter in the fundamental loop allows moving the gating window along an entire laser period for a coarse control of the relative position of the pulses, while the fine positioning is obtained by moving the motorized delay lines transporting the reference signal to the harmonic loops.

To achieve better performances, especially in the phase detection process, we need to migrate towards optical reference signal distribution architecture. We have already purchased and installed an Optical Master Oscillator (OMO), which is presently under test. Also we have partially installed the fiber links to bring the signal to the clients (laser oscillators, RF power station, diagnostics). Next step is to characterize the high resolution optical phase detectors (cross-correlators) that will guarantee a minimal time jitter resolution of the order of 1 fs.

To guarantee a stable operation in both electrical and optical reference signal distribution, we are designing the system including a link stabilization apparatus. The optical stabilized links are nowadays available on the market, providing residual drifts of the order of 10 fs_{RMS} in point-to-point reference distribution. Concerning the coaxial cable distribution, we are developing a link monitor that can diagnose the drifts of the signal path length. We will use this information to close a pulse-to-pulse feedback loop, compensating the drift using the motorized delay lines.

5. Advanced beam dynamics experiments

With the SPARC photoinjector a new technique called Laser Comb [10], aiming to produce a train of short electron bunches, has been tested [14]. In this operating mode, the photocathode is illuminated by a comb-like laser pulse to extract a train of electron bunches injected into the same RF bucket of the gun. The SPARC_laser system, based on a Ti:Sa oscillator has been upgraded for this specific application. The technique used relies on a α-cut beta barium borate (α-BBO) birefringent crystal, where the input pulse is decomposed in two orthogonally polarized pulses with a time separation proportional to the crystal length. In the first accelerating structure operating in the VB mode, i.e., injecting the bunch train near the zero crossing of the RF wave, the bunch train is compressed by the longitudinal focusing effect of the RF wave. Moreover, with a proper choice of injection phase it becomes possible

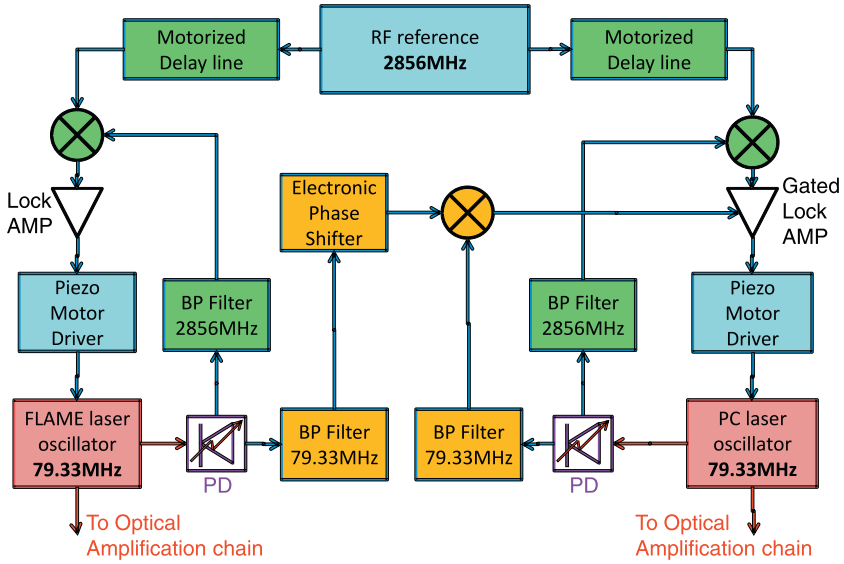

Fig. 5. Sketch of the lasers synchronization scheme used in the Thomson scattering experiment.

to keep under control both intra-bunch distance and single bunch length. This method preserves all extracted charge and it is different from other passive techniques [15], where the train is produced by using a mask that stops a significant fraction of the charge. Up to four electron beam pulses shorter than 300 fs and separated by less than 1 ps have been characterized and a narrowing THz spectrum produced by the bunch train has been measured [8]. In addition two electron beam pulses have been injected in the undulator and a characteristic interference spectrum produced by the FEL interaction in this new configuration has been observed. That confirms that both pulses have been correctly matched to the undulator and was both lasing [16]. Coherent excitation of plasma waves in plasma accelerators [15] can be also performed with this technique. Preliminary simulations [17] have shown that a train of three electron drive bunches, each of them 25 μm long, with 200 pC at 150 MeV and 1 μm rms normalized emittance, could accelerate up to 250 MeV a 20 pC, 10 μm long witness bunch, injected at the same initial energy in a 10 cm long plasma of wavelength 383 μm. As shown in Fig. 6, the drive bunches will lose energy to excite the plasma accelerating field up to 1 GV/m in favor of the witness bunch. Simulations show also that the witness bunch can preserve a high quality with a final energy spread less than 1% and 1.6 μm rms normalized emittance. A test experiment is foreseen at SPARC_LAB, aiming to produce a high quality plasma accelerated beam able to drive a FEL in the SASE mode.

In addition to the PWFA experiment, another configuration of plasma acceleration is foreseen at SPAR_LAB. It exploits the LWFA scheme. The compressed laser pulse of FLAME excites a plasma wave, and a bunch produced by SPARC is injected in the trailing area at a proper distance from the laser pulse. The plasma wavelength must be long enough to allow an easy injection, i.e. an accurately chosen time of arrival of the electron bunch. Moreover, since the e-bunches can not be arbitrarily short, in order to reduce the final energy spread, the accelerating field curvature shell be small on the bunch length scale. This means longer plasma wavelength and, in turn, an average accelerating field, which will be much lower than the one produced in self-injection experiments (up to 1 TV/m) due to the fact that the plasma density will be up to some 10^{17} cm^{-3}, producing a filed intensity in the range of few to few tens of GV/m.

To yield a significant increase of the bunch energy, the active accelerating length shall then be in the order of few to few tens of cm, which is much longer than the typical Rayleigh length of a laser pulse. This means a device capable of driving the laser pulse is needed. Our choice is to employ a glass capillary with an internal diameter ranging from about 50 up to 200 or more μm. A leakage of laser energy is foreseen from the capillary inner surface, but it can be shown to be negligible or tolerable for a wide range of inner capillary diameters of practical interest [20].

As a starting working set up we chose a capillary internal diameter of D_{cap} = 200 μm, which should represent a relaxed target for pointing issues, and a plasma density $n_0 = 10^{17}$; With D_{cap} being large, the expected characteristic decaying length for the laser energy is larger than 7 m. The expected laser energy at the capillary entrance is up to 3.5 J. Preliminary simulations show that it is possible to excite an almost (longitudinally) linear plasma wave with an average accelerating field of about 1.8 GV/m. Assuming a capillary length of 20 cm, the accelerated electron beam possesses fairly good overall properties assuming the injected bunch has the global parameters reported in Table 1.

An extensive simulation campaign is ongoing in order to asses other interesting working points, enabling to reach energies in the order of GeV, while preserving the beam brightness. To this end, a sound procedure to match the bunch from the plasma channel to vacuum, at the capillary end, is in need, preventing the unacceptable normalized emittance dilution foreseen in [21]. Switching to a mild non-linear regim will produce more intense accelerating fields. The trade-off is a larger field curvature and a higher energy spread. In such a set up, an increase of the bunch charge could develop a quite large amount of beam loading that can be used, if the bunch is properly injected, to mitigate the curvature driven energy spread [19].

6. Thz source

The motivation for developing a linac-based THz source at SPARC_LAB stays in the ever growing interest of filling the so-called THz gap with high peak power radiation. From simulations, the peak power expected at SPARC is in the order of 10^8 W. This result has been confirmed by measurements presented in [22]. The corresponding energy per pulse is of the order of tens of μJ that is well above standard table top THz sources.

Applications of this kind of source concern mainly time domain THz spectroscopy and frequency domain measurements on novel

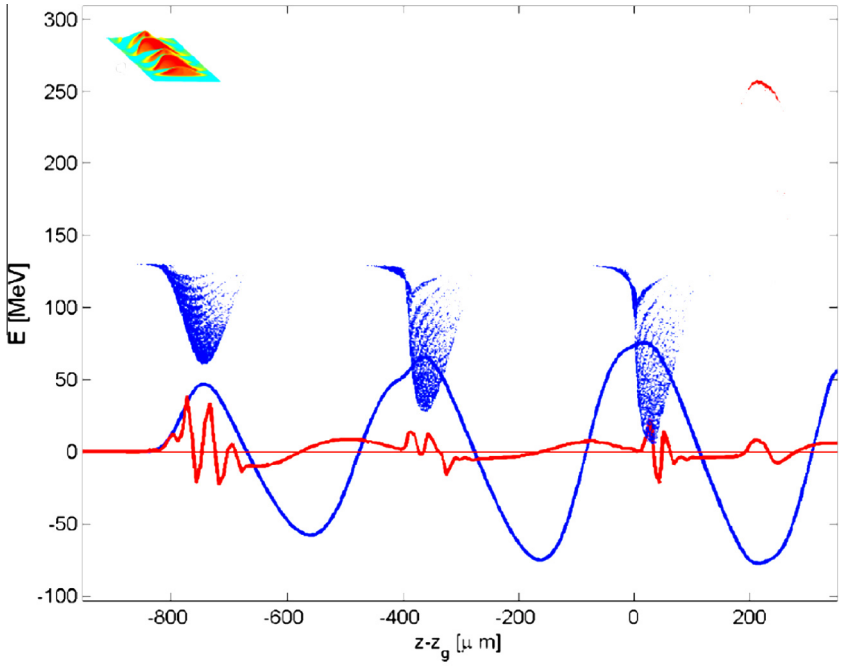

Fig. 6. Longitudinal phase space of the COMB beam at the end of the acceleration process. The accelerating field is also plotted in arbitrary units.

Table 1
LWFA expected parameters.

	Plasma entrance	Plasma exit
Charge	5 pC	5 pC
σ_{tr}	10 μm	3.6 μm
σ_z	3.5 μm	3.5 μm
$\Delta\gamma/\gamma$	10^{-3}	5 10^{-2}
Energy	160 MeV	565 MeV

Table 2
THz source achieved performances.

Energy per pulse (μJ)	~10
Peak power (MW)	100
Average power (W)	2×10^{-4}
Electric field (kV/cm)	>100
Pulse duration (fs)	<200

materials [23]. Beyond these applications, coherent THz radiation is also used as longitudinal electron beam diagnostics to reconstruct the beam charge distribution [24].

In addition, taking advantage from electron beam manipulation techniques, high power, narrow-band THz radiation can be also generated at SPARC_LAB. This provides a unique chance to realize, with the SPARC THz source, THz-pump/THz-probe spectroscopy, a technique practically unexplored up to now.

The source is both Coherent Transition Radiation (CTR) from an aluminum coated silicon screen and Coherent Diffraction Radiation (CDR) from a rectangular cut on the screen. The screen is placed in the vacuum pipe at the end of the by-pass, at 45° with respect to the electron beam direction. Two branches are installed: one for interferometer measurements and one for integrated CTR/CDR measurements with the possibility of selecting custom band pass filters in the THz range.

CTR/CDR is emitted by both an ultra-short high-brightness electron beam and a longitudinally modulated one, based on the combination of velocity bunching and laser comb techniques. Depending on the working point of the accelerator, the THz radiation can be tuned in order to optimize different characteristics. So far achieved THz radiation performances, through CTR generated by a single bunch (500 pC, 500 fs with 110 MeV energy) are reported in Table 2.

7. Electron crystal channeling and applications

Recently we have started with a new project POSSO on studying the features of moderate-energies (0.1–1 GeV) electron beam channeling in various crystals [25]. The project aims in creating for a SPARC_LAB group both knowledge and experience for applying orientational behaviours of charged particles passage through the crystals to shape the beams (beam bending, collimation) as well as to generate a powerful X-ray and γ-radiation source (coherent bremsstrahlung, channeling radiation, parametric X-ray radiation) [26]. One of the most interesting channeling-based application is a technique originated on its optimized combination with conventional methods for positron sources; electron channeling, namely channeling radiation by ultrarelativistic electrons (>1 GeV) in crystals, is rather promising for getting high brilliant positron beams for the future e^-/e^+ colliders (see Figs. 7 and 8).

Within the project we have performed theoretical studies that finalized in new computer codes for planar and axial channeling of relativistic electrons in various types of the crystals, detailed analysis of orientation features of electron scattering at axial channeling in very thin (submicron) monocrystals (studies on mirror reflection of the beam), detailed analysis of electron dechanneling and rechanneling at planar case based on solution of Fokker–Plank equations, getting the radiation power behind the crystals at the channeling orientations for various emittance parameters of the beam before the crystal, and electron beam simulations by the GEANT4-based codes for the optimization of experimental layout.

With the increase of electron energy the radiation loss due to the beam channeling becomes essential; for instance, for the electron energy change from 150 MeV to 200 MeV the radiation intensity in Si(1 1 0) increases two times, while for 800 MeV electrons the radiation flux becomes one order higher. Keeping in mind that the depth of a Si(1 1 0) potential well (~20 eV) is much less deeper than the one for a W⟨1 0 0⟩(~800 eV), we can expect extremely

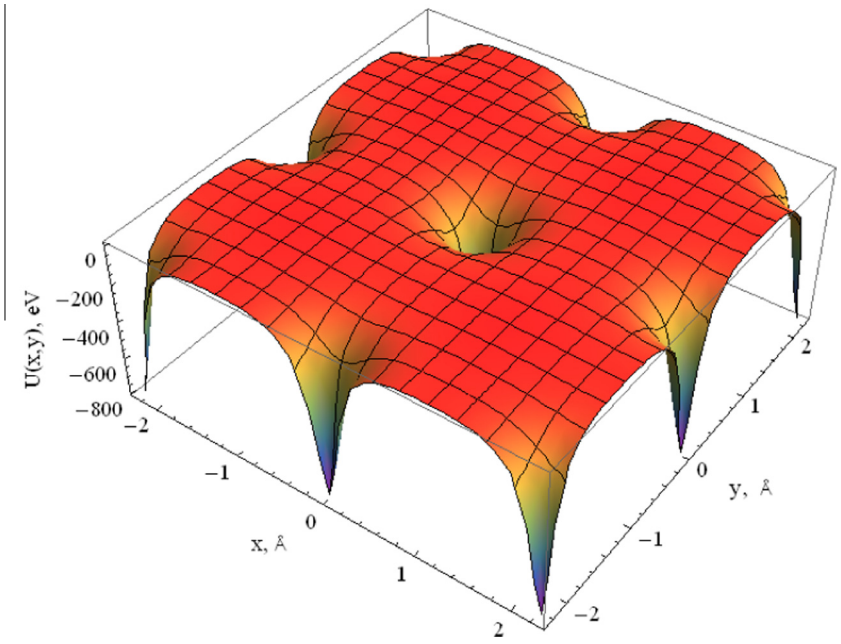

Fig. 7. The averaged potential energy of electron interaction with W⟨100⟩ crystallographic axis within the Doyle–Turner approximation. Due to extremely high gradient of the potential well 10^2–10^3 GeV/m we can expect high flux of channeling radiation [26] .

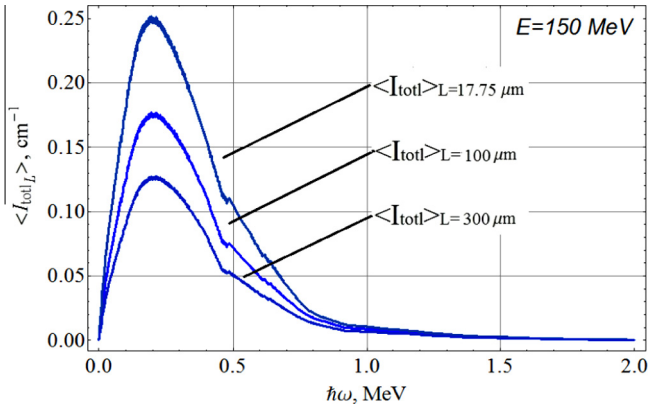

Fig. 8. Total radiation yield of channeling radiation by single electron per unit of a Si⟨110⟩ crystal length for three various crystal thicknesses. In final design the thickness should be optimized.

high channeling radiation flux in W to be emitted witin the cone of the angular width $1/\gamma \sim 10^{-3}$ [26]. Additionally, together with the SPARC_LAB team we have evaluated various possible solutions for a new beam line dedicated to channeling studies, and, finally, have chosen the layout to be constructed as a continuation of the dogleg piece of the THz beamline.

References

[1] D. Alesini et al., Nucl. Instr. Meth. A 507 (2003) 345.
[2] D. Giulietti et al., Proceeding of PAC, Knoxville, Tennessee, USA, 2005.
[3] M. Ferrario et al., Phys. Rev. Lett. 99 (2007) 234801.
[4] M. Ferrario et al., Phys. Rev. Lett. 104 (2010) 054801.
[5] L. Giannessi et al., Phys. Rev. Lett. 106 (2011) 144801.
[6] M. Labat et al., Phys. Rev. Lett. 107 (2011) 224801.
[7] L. Giannessi et al., Phys. Rev. Lett. 108 (2012) 164801.
[8] E. Chiadroni et al., J. Phys: Conf. Ser. 357 (2012) 012034.
[9] L.A. Gizzi et al., Europ. Phys. J. – Special Topics 175 (2009) 3.
[10] M. Ferrario et al., Nucl. Instr. Meth. A 637 (1) (May 2011) S43–S46.
[11] P. Oliva et al., Nucl. Instr. Meth. A 615 (2010) 93–99.
[12] A. Bacci et al., Nucl. Instr. Meth. A 608 (2009) S90–S93.
[13] U. Bottigli et al., Il Nuovo Cimento 29C (N.2) (2006).
[14] A. Mostacci et al., TUPPD055, These Proceedings.
[15] P. Muggli, Proc. of PAC 2009, Vancouver, Canada.
[16] A. Bacci et al., Proceedings of FEL Conference 2011, Shanghai, China, 2011.
[17] P. Tomassini, Private Communication.
[18] C. Vaccarezza, TUOBB01, These Proceedings.
[19] A.R. Rossi, WEEPPB002, These Proceedings.
[20] B. Cross et al., Phys. Rev. E 65 (2002) 026405.
[21] P. Antici et al., J. Appl. Phys. 112 (2012) 044902.
[22] E. Chiadroni et al., Proceedings of IPAC 2010, TUOARA03, Kyoto, 2010.
[23] M.S. Sherwin et al., Opportunities in THz Science, Report of a DOE-NSF-NIH, Workshop (2004).
[24] E. Chiadroni et al., Rev. Sci. Instr. 84 (2013) 022703.
[25] S.B. Dabagov, N.K. Zhevago, La Rivista del Nuovo Cimento 31 (9) (2008) 491.
[26] S.B. Dabagov et al., IJMPh A 22 (23) (2007) 4280.